



# Momentum Distribution of Nucleons in Isospin Asymmetric Nuclear Matter

Javier Rufino<sup>1,2</sup>, Jeremy Holt<sup>2</sup>

1. Department of Physics and Astronomy, University of Texas at San Antonio, San Antonio, TX 78249
2. Cyclotron Institute, Texas A&M University, College Station, TX 77843



The University of Texas at San Antonio  
Department of Physics and Astronomy



## Motivation

Neutron stars are the densest observable objects in the universe and consist primarily of neutron rich nuclear matter in a background of ultra-relativistic electrons. They maintain stability from gravitational collapse with the support of the quantum mechanical degeneracy pressure and nuclear interactions. To better understand the effects of nuclear short-range correlations on neutron star structure and dynamics we compute the single-particle momentum distribution of protons and neutrons starting from high precision two- and three-body forces derived from chiral effective field theory.

## Methods

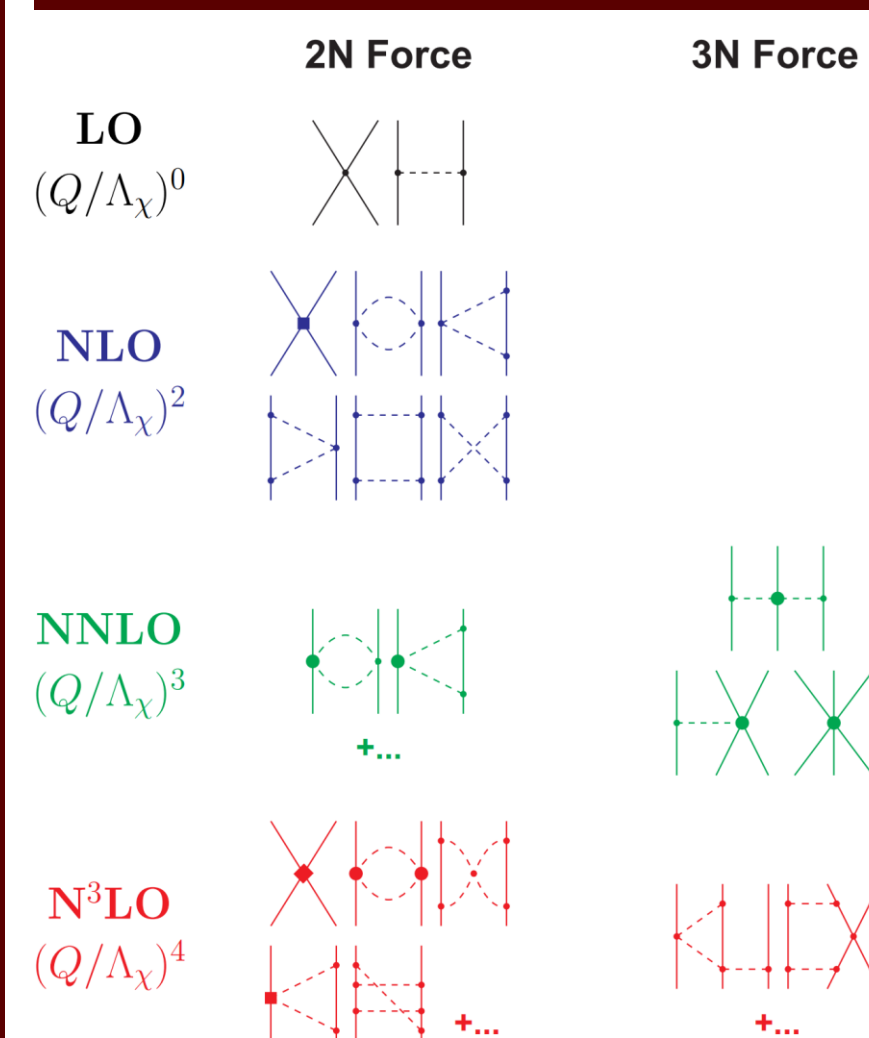


**Figure 1:** The diagrams in this figure are taken from Machleidt et al.<sup>4</sup> and represent the contributions to nuclear two-body and many-body forces. The solid lines represent nucleons and the dashed lines pions.

- From chiral effective field theory two- and three- body forces we computed the first- and second-order contributions to the nucleon self-energies.
- These self-energies are dependent on spin, isospin, momentum and density ( $\Sigma_{p,n}^{(2a,2b)}(q,\omega;k_f,\delta_{pn})$ ), and once computed are summed up to produce single-particle potentials ( $V_{(q,e(q))} = \text{Re} \Sigma_{(q,e(q))}$ ), of which are used to compute the momentum distribution.
- The nucleon self-energies were computed using the Texas A&M University supercomputer Terra. The following computations were done on C and Mathematica, and graphed on Mathematica.

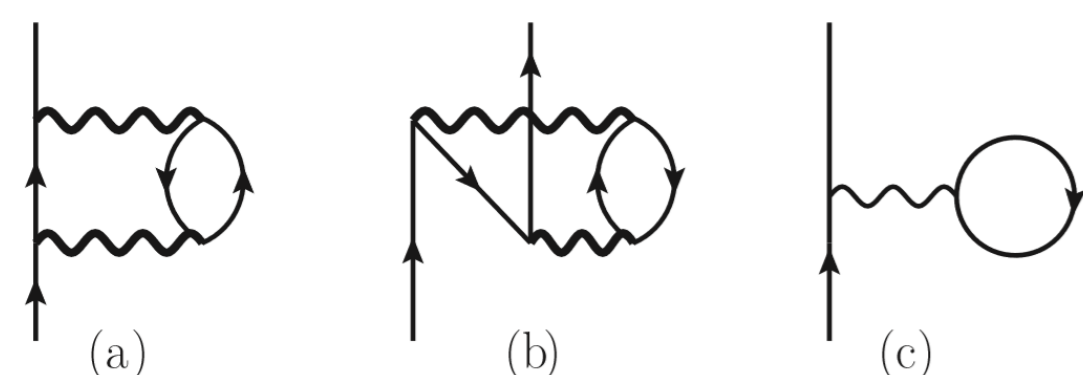


**Figure 2:** The first order and second order contributions of the nucleon self energies are represented diagrammatically provided by Holt et al<sup>1</sup>. The arrows pointing upwards and downwards represent nucleons, and hole states, respectively. The wavy line represents anti-symmetrized two nucleon interaction, and the thick wavy lines represent the sum of the free-space two-body force and the density dependent NN interaction.

## Single-Particle Momentum Distribution

Using the equations derived in the work of Sartor et al., we were able to compute the momentum distribution from our single-particle potentials. The following momentum distributions have been computed for values up to twice the nuclear saturation density, and arbitrary values of isospin asymmetries,  $\delta_{np} = (N - Z)/A$ .

$$\frac{\bar{m}_{(q)(2a)}}{m} = 1 - \frac{\partial V_{(q,E)(2a)}}{\partial E} \Big|_{E=\frac{q^2}{2m} + \text{Re} \Sigma_{(q,e(q))}}$$

$$\frac{\bar{m}_{(q)(2b)}}{m} = 1 - \frac{\partial V_{(q,E)(2b)}}{\partial E} \Big|_{E=\frac{q^2}{m} + \text{Re} \Sigma_{(q,e(q))}}$$

$$\rho_{(q)} = \begin{cases} 2 - \frac{\bar{m}_{(q)(2a)}}{m}, & \text{for } q < q_f \\ \frac{\bar{m}_{(q)(2b)}}{m} - 1, & \text{for } q > q_f \end{cases}$$

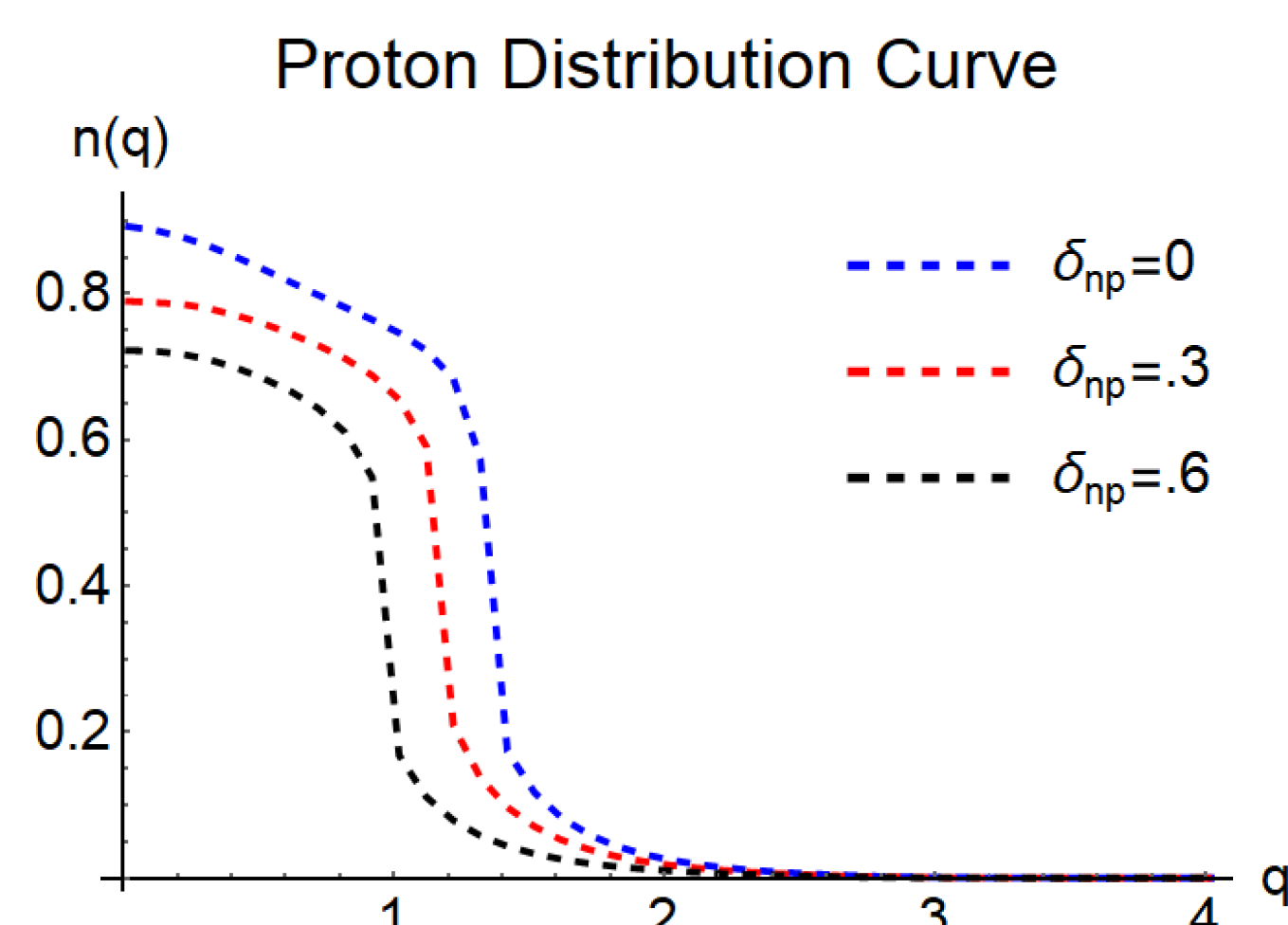


**Figure 3:** The momentum distribution of a proton under three arbitrary isospin asymmetries, and the nuclear saturation density  $\rho = .16$

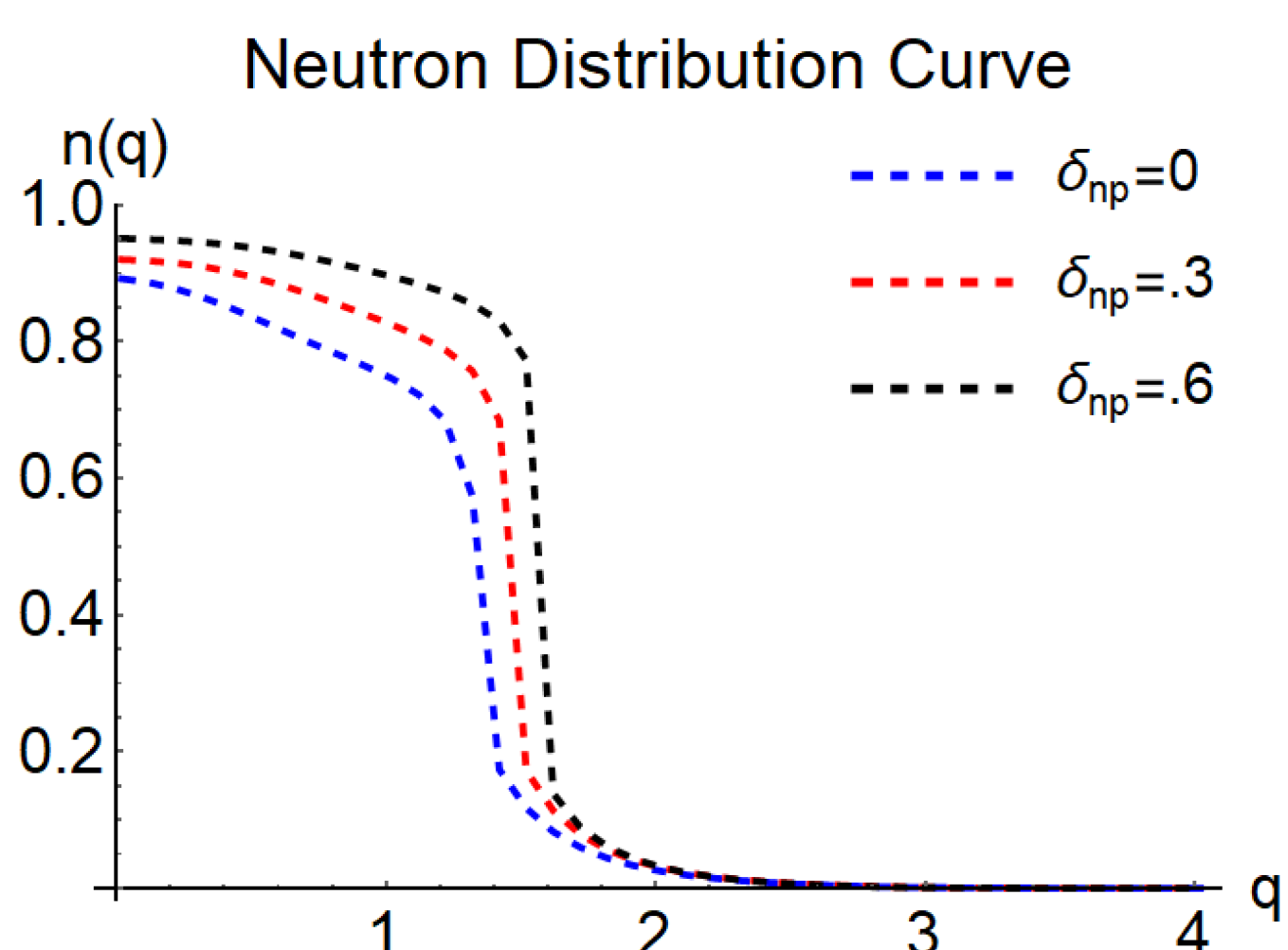


**Figure 5:** The momentum distribution of a neutron under three arbitrary isospin asymmetries, and the nuclear saturation density  $\rho = .16$

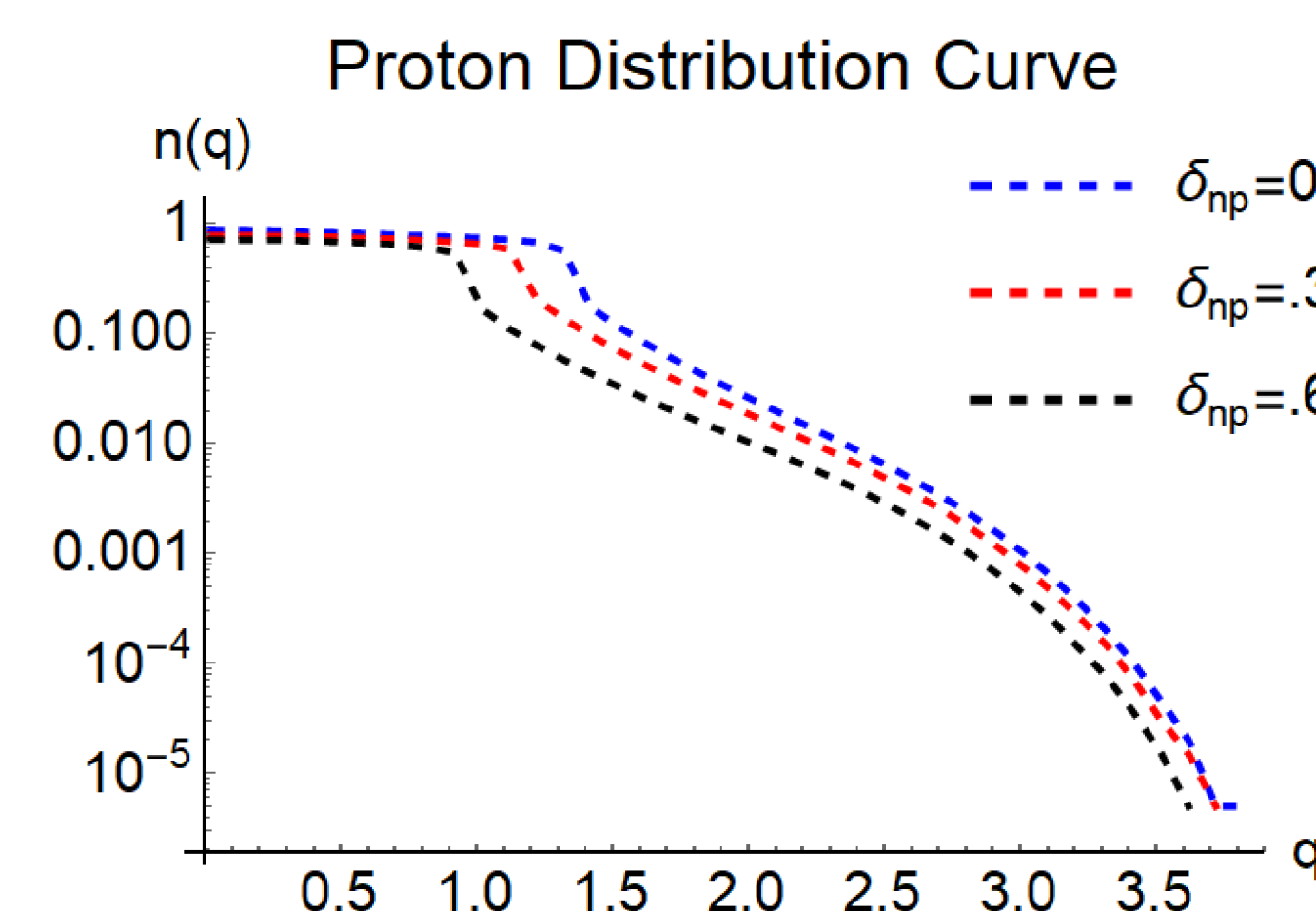


**Figure 4:** Logarithmic plot of figure 2, used to have a visual focus on the tail end of the plot.

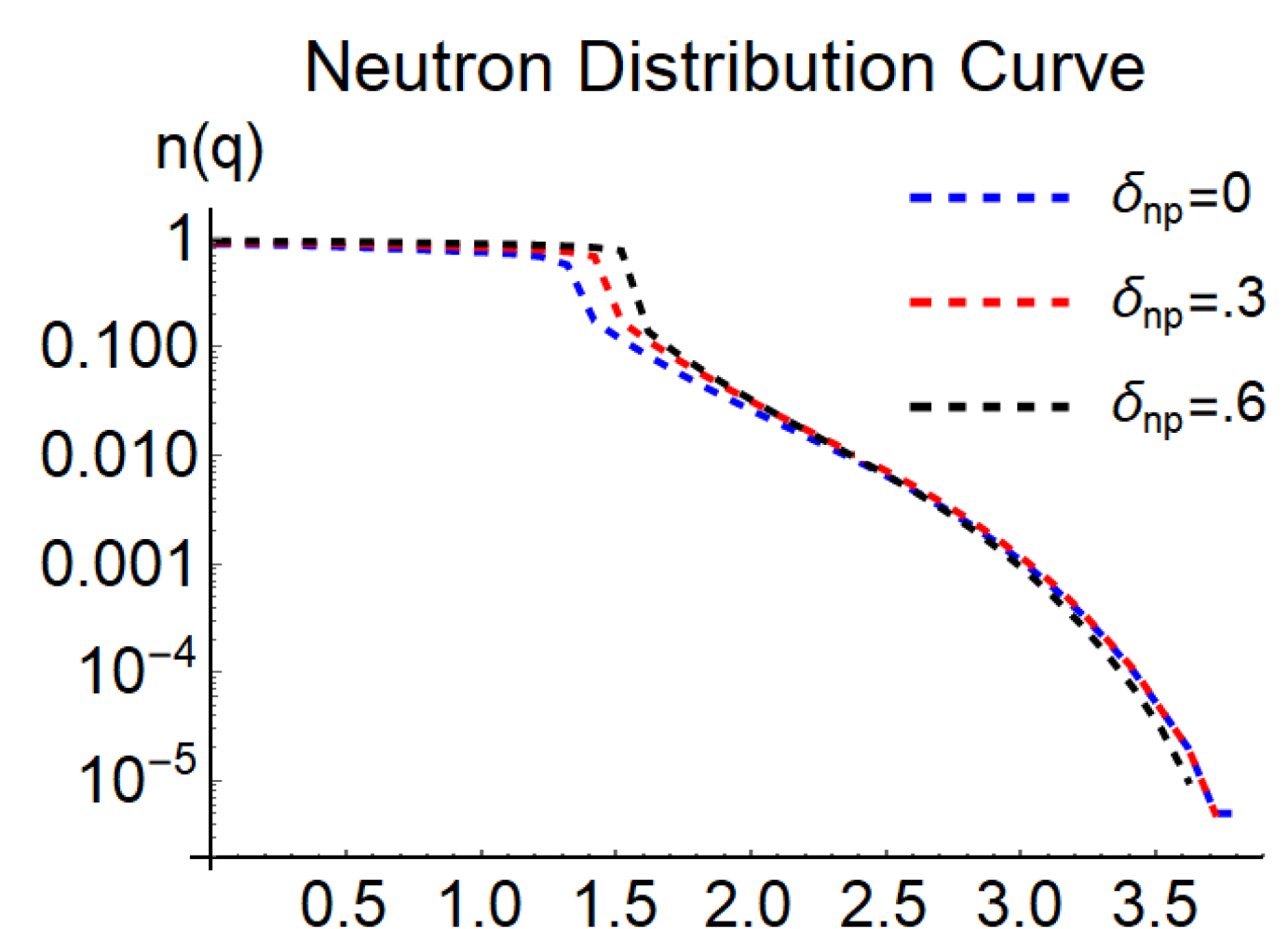


**Figure 6:** Logarithmic plot of figure 3, used to have a visual focus on the tail end of the plot.

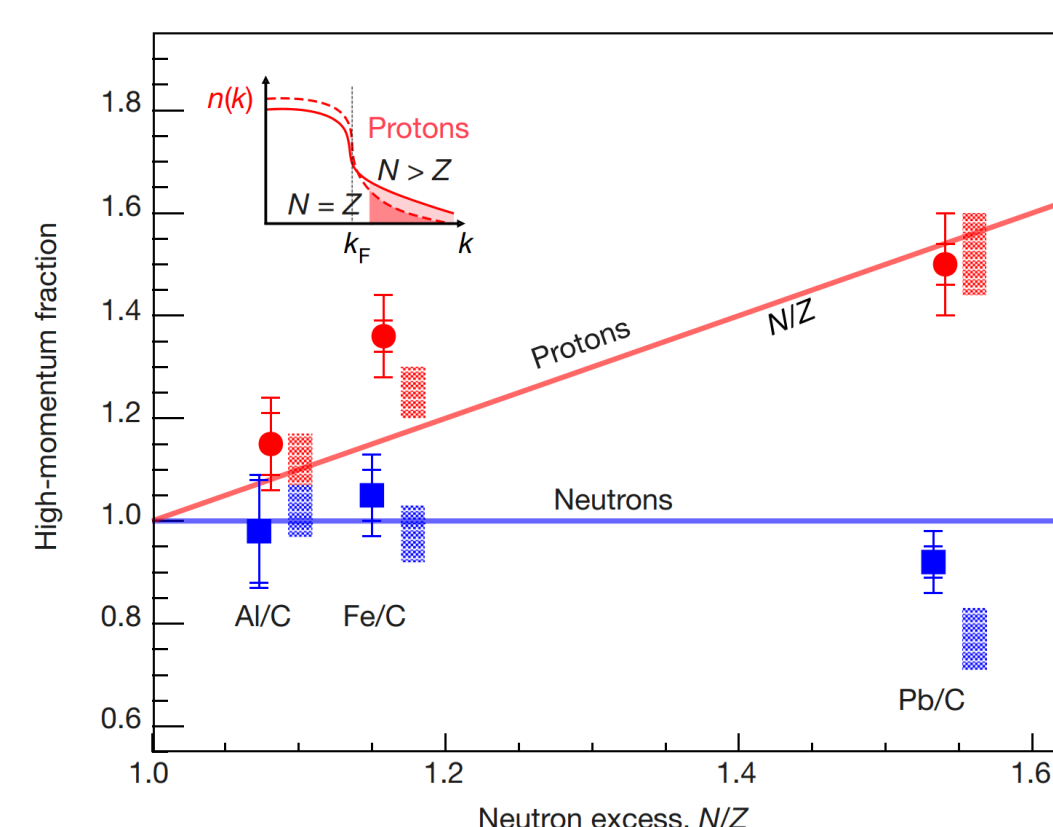


**Figure 7:** This figure is taken from a collaboration project of CLAS<sup>2</sup>.

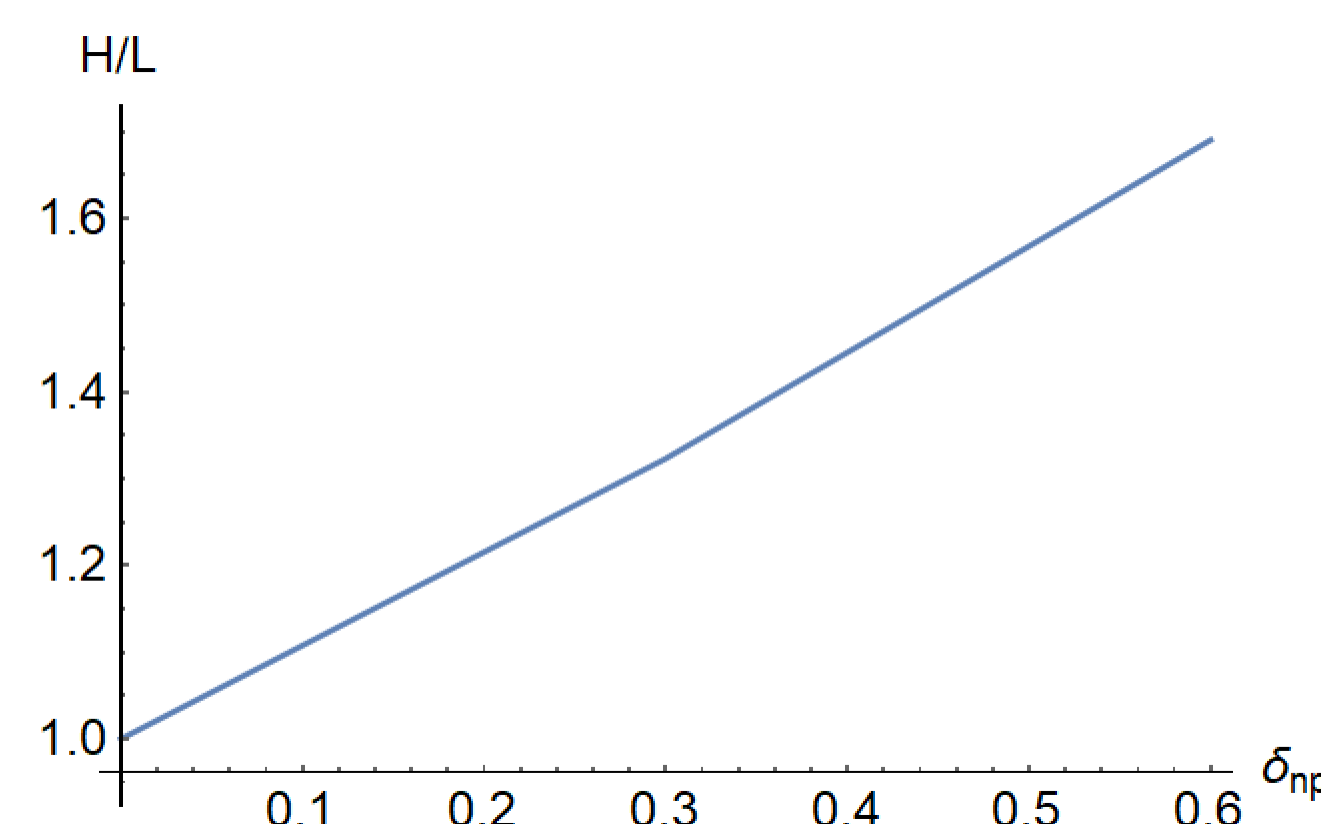


**Figure 8:** A plot showing the linear relationship between high momentum fractions vs neutron excess, similar to experimental data seen in **Figure 7**.

## Discussion

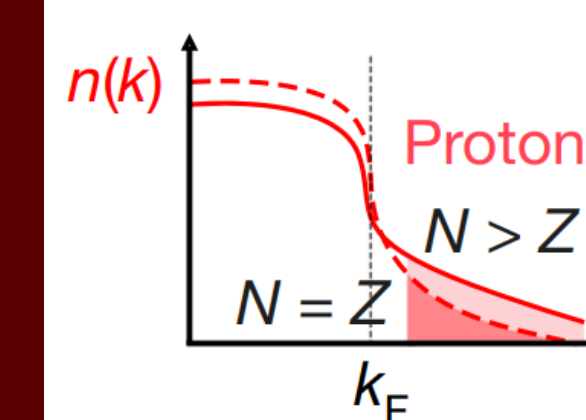
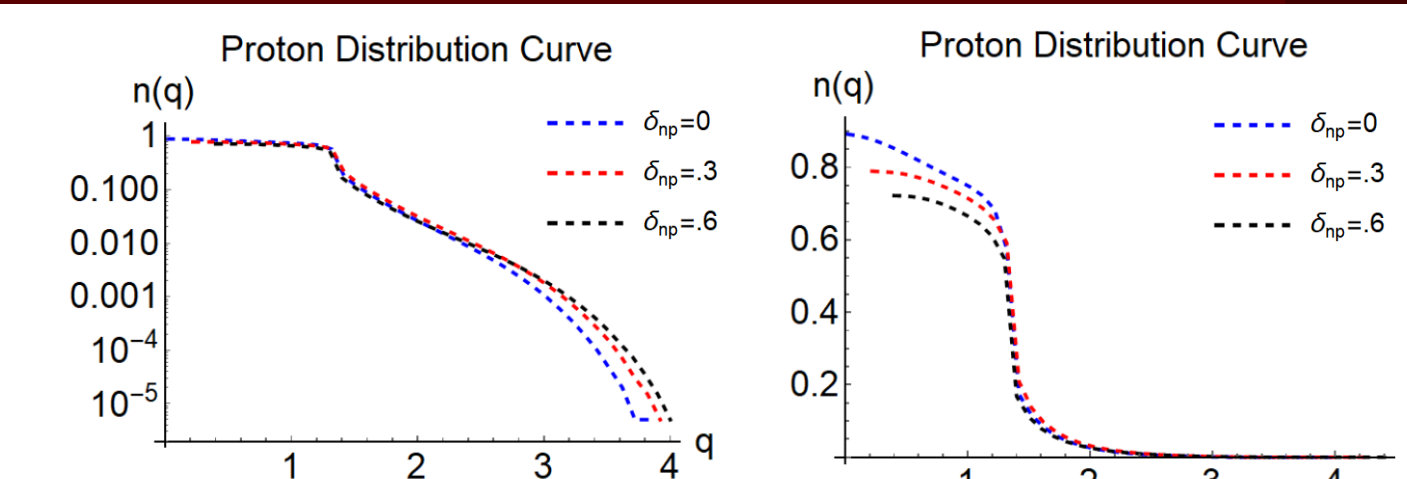


**Figure 9:** This figure taken from a collaboration project of CLAS<sup>2</sup>, and is an inset from **Figure 7**.



**Figures 10 & 11:** These figures are the same graph as **Figures 3 & 4** with horizontal shifts in the curves with isospin asymmetries  $\delta_{np} = 0.3$  and  $0.6$ .

The inset in the experimental data (**Figure 8**) provides a proton momentum distribution of neutron rich scattered nuclei. The experimental data states that as isospin asymmetry in a given nuclei increases, the ratio of high momentum protons to low-momentum protons also increases. We observe that our theoretical calculations also exhibit an increase in the proton high-momentum tail for isospin-asymmetric systems.

	$\delta_{np}=0.0$	$\delta_{np}=0.3$	$\delta_{np}=0.6$
High-Momentum States	0.342/0.342=1.0	0.453/0.342=1.3	0.578/0.342=1.7
Low-Momentum States			

## Conclusion and Future works

The present work demonstrates that theoretical calculations of nucleon momentum distributions in asymmetric nuclear matter from realistic two- and three-body chiral nuclear forces reproduce trends observed in experimental (e,e'p) and (e,e'n) reactions. In the future we will consider the role of nuclear short-range correlation on neutrino scattering rates in neutron stars

## References

1. J. W. Holt. Microscopic optical potential for exotic isotopes from chiral effective field theory, 10.1103/PhysRevC.93.064603
2. Nature 560. Probing high-momentum protons and neutrons in neutron-rich nuclei. (2018, August 13), <https://doi.org/10.1038/s41586-018-0400-z>
3. Sartor, R., and C. Mahaux. "Self-Energy, Momentum Distribution, and Effective Masses of a Dilute Fermi Gas." *Physical Review C*, vol. 21, no. 4, 1980, pp. 1546–1567, doi:10.1103/physrevc.21.1546.
4. Machleidt, R., and D.r. Entem. "Chiral Effective Field Theory and Nuclear Forces." *Physics Reports*, vol. 503, no. 1, 2011, pp. 1–75, doi:10.1016/j.physrep.2011.02.001.

## Acknowledgements

- I would like to acknowledge Dr. Jeremy Holt for his guidance and support throughout this project.
- I would like to acknowledge this work being supported by the NSF grant number PHY-1659847